

## Borohydride Anions as Terminal Ligands on a Fe/Mo/S Cluster. Synthesis, Structure, and Characterization of the [(Cl<sub>4</sub>-cat)(PPR<sub>3</sub>)MoFe<sub>3</sub>S<sub>4</sub>(BH<sub>4</sub>)<sub>2</sub>]<sub>2</sub>(Bu<sub>4</sub>N)<sub>4</sub> Double-Fused Cubane

Markos Koutmos and Dimitri Coucouvanis\*

Department of Chemistry, The University of Michigan, Ann Arbor, Michigan 48109

Received June 3, 2004

The synthesis and structure of the first Mo/Fe/S/BH<sub>4</sub> cluster is reported. Reaction of (Cl<sub>4</sub>-cat)<sub>2</sub>Mo<sub>2</sub>Fe<sub>6</sub>S<sub>8</sub>(PPR<sub>3</sub>)<sub>6</sub> with 4 equiv of Bu<sub>4</sub>NBH<sub>4</sub> results in the formation of [(Cl<sub>4</sub>-cat)(PPR<sub>3</sub>)MoFe<sub>3</sub>S<sub>4</sub>(BH<sub>4</sub>)<sub>2</sub>]<sub>2</sub>(Bu<sub>4</sub>N)<sub>4</sub> (Cl<sub>4</sub>-cat = tetrachloro-catecholate) which has been fully characterized. X-ray structural determination of this double-fused cubane reveals four BH<sub>4</sub><sup>-</sup> ligands bound to four Fe atoms in a bidentate fashion. A synopsis of the solution characterization as well as the reactivity of this cluster is also presented.

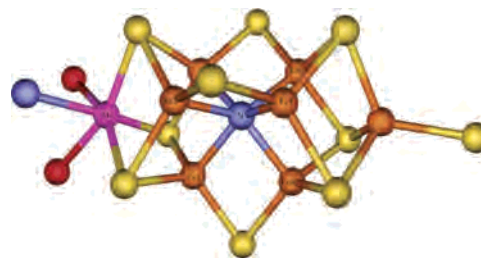


Figure 1. Structure of the FeMoS center of nitrogenase.

Single crystal structure determinations of the Mo–Fe protein of nitrogenase have revealed the unique structure of the FeMoS cofactor, FeMoco (Figure 1).<sup>1</sup>

Exact synthetic analogues for the nitrogenase FeMo cofactor are not available; however, clusters with MoFe<sub>3</sub>S<sub>4</sub><sup>4</sup> and MoFe<sub>3</sub>S<sub>3</sub><sup>5</sup> cuboidal subunits are known and have contributed significantly to fundamentally important chemistry. The mechanism of dinitrogen activation and reduction by the FeMoS cofactor in nitrogenase has been the subject of numerous calculations and suggestions.<sup>6</sup> The variety of theoretical models available underscores the fact that the mechanism of N<sub>2</sub> fixation is still an unresolved problem. The

nitrogenase enzyme also has hydrogenase activity reducing H<sup>+</sup> to H<sub>2</sub> which acts as an inhibitor to NH<sub>3</sub> formation. A mechanism that involves the possible formation of FeMoco–hydrogen or –hydride intermediates has been described recently.<sup>7</sup> To test the possible existence of these proposed metallo-hydrido or hydrogen atom clusters, we investigated the reactions of MoFeS clusters with hydride sources such as BH<sub>4</sub><sup>-</sup> anions.

In this paper, we report on the synthesis and structure of a new FeMoS cluster that contains BH<sub>4</sub><sup>-</sup> ligands.

The cluster [(Cl<sub>4</sub>-cat)(PPR<sub>3</sub>)MoFe<sub>3</sub>S<sub>4</sub>(BH<sub>4</sub>)<sub>2</sub>]<sub>2</sub>(Bu<sub>4</sub>N)<sub>4</sub>, **I**, is obtained from the reaction between (Cl<sub>4</sub>-cat)<sub>2</sub>Mo<sub>2</sub>Fe<sub>6</sub>S<sub>8</sub>(PPR<sub>3</sub>)<sub>6</sub>, **IIa**,<sup>3</sup> and Bu<sub>4</sub>NBH<sub>4</sub> in 85% yield<sup>8</sup> (Cl<sub>4</sub>-cat = tetrachloro-catecholate; [(Cl<sub>4</sub>-cat)<sub>2</sub>Mo<sub>2</sub>Fe<sub>6</sub>S<sub>8</sub>(PPR<sub>3</sub>)<sub>6</sub>], **II** (where R = <sup>n</sup>Pr, **IIa**; Et, **IIb**; <sup>n</sup>Bu, **IIc**)). This reaction proceeds in THF at ambient temperatures and goes to completion after overnight stirring. Crystals of **I** are obtained following dilution with a mixture of diethyl ether and hexanes at room temperature.<sup>9</sup>

The crystal structure of **I**, Figure 2, reveals the metal sulfur cluster in an arrangement where two edge-sharing MoFe<sub>3</sub>S<sub>4</sub> “cubane” units define an octanuclear cluster as in clusters **IIb** and **IIc**.<sup>3</sup> Due to the lack of good structural data for compound **IIa**, [(Cl<sub>4</sub>-cat)<sub>2</sub>Mo<sub>2</sub>Fe<sub>6</sub>S<sub>8</sub>(PEt<sub>3</sub>)<sub>6</sub>], **IIb**, and [(Cl<sub>4</sub>-

\* To whom correspondence should be addressed. E-mail: dcouc@umich.edu.

- (1) (a) Kim, J.; Rees, D. C. *Science*, **1992**, *257*, 1677. (b) Howard, J. B.; Rees, D. C. *Chem. Rev.* **1996**, *96*, 2965. (c) Einsle, O.; Tezcan, A. F.; Andrade, S. L. A.; Schmid, B.; Yoshida, M.; Howard, J. B.; Rees, D. C. *Science* **2002**, *297*, 1696–1700. (d) Bolin, J. T.; Ronco, A. E.; Morgan, T. V.; Mortenson, L. E.; Xuong, N. H. *Proc. Natl. Acad. Sci. U.S.A.* **1993**, *90*, 1078. Georgiadis, M. M.; Komiyama, H.; Woo, D.; Kornuc, J. J.; Rees, D. C. *Science* **1992**, *257*, 1653.
- (2) (a) Malinak, S. M.; Coucouvanis, D. *Prog. Inorg. Chem.* **2001**, *49*, 599 and references therein. (b) Lee, S. C.; Holm, R. H. *Chem. Rev.* **2004**, *104*, 1135 and references therein.
- (3) (a) Han, J.; Koutmos, M.; Al Ahmad, S.; Coucouvanis, D. *Inorg. Chem.* **2001**, *40*, 5985. (b) Demadis, K. D.; Campana, C. F.; Coucouvanis, D. *J. Am. Chem. Soc.* **1995**, *117*, 7832.
- (4) (a) Osterloh, F.; Segal, B. M.; Achim, C.; Holm, R. H. *Inorg. Chem.* **2000**, *39*, 980. (b) Osterloh, F.; Achim, C.; Holm, R. H. *Inorg. Chem.* **2001**, *40*, 224.
- (5) (a) Coucouvanis, D.; Han, J.; Moon, N. *J. Am. Chem. Soc.* **2002**, *124*, 216. (b) Tyson, M. A.; Coucouvanis, D. *Inorg. Chem.* **1997**, *36*, 3808.
- (6) (a) Hinneman, B.; Nørskov, J. K. *J. Am. Chem. Soc.* **2003**, *125*, 1466. (b) Dance, I. *Chem. Commun.* **2003**, 324. (c) Lovell, T.; Liu, T.; Case, D. A.; Noodleman, L. *J. Am. Chem. Soc.* **2003**, *125*, 8377. (d) Schimpl, J.; Petrill, H. M.; Blochl, P. E. *J. Am. Chem. Soc.* **2003**, *125*, 15772.

(7) Huniar, U.; Ahlrichs, R.; Coucouvanis, D. *J. Am. Chem. Soc.* **2004**, *126*, 2588.

(8) Elemental microanalysis calcd for C<sub>94</sub>H<sub>202</sub>B<sub>4</sub>Cl<sub>8</sub>Fe<sub>6</sub>Mo<sub>2</sub>N<sub>4</sub>O<sub>4</sub>P<sub>2</sub>S<sub>8</sub>: C, 43.01; H, 7.76; N, 2.13. Found: C, 43.12; H, 7.67; N, 2.06. IR (KBr pellet, cm<sup>-1</sup>): B–H, 2363(m), 2291(m), 2224(m), 2085(m); Cl<sub>4</sub>-Cat, 1439(vs). Magnetic susceptibility (solid): μ<sub>eff</sub> (2 K) 5.583 μB, μ<sub>eff</sub> (300 K) 7.315 μB. EPR (solid): silent.

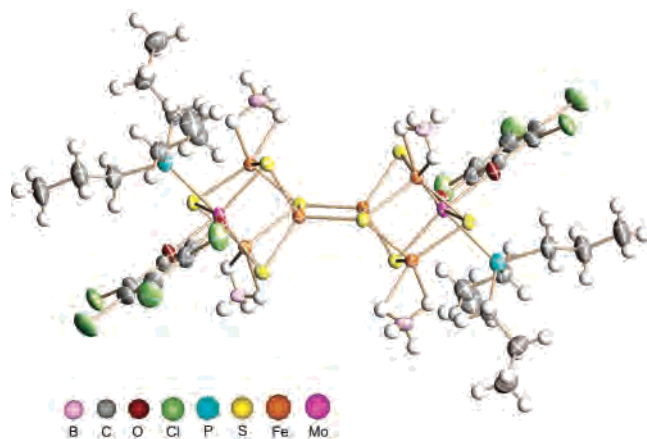


**Figure 2.** ORTEP diagram of the  $[(\text{Cl}_4\text{-cat})(\text{PPr}_3)\text{MoFe}_3\text{S}_4(\text{BH}_4)_2](\text{Bu}_4\text{N})_4$  (**I**) cluster showing the thermal ellipsoids. The  $\text{Bu}_4\text{N}^+$  cations have been omitted for clarity.

$\text{cat})_2\text{Mo}_2\text{Fe}_6\text{S}_8(\text{P}^n\text{Bu}_6)_6$ , **IIc**, have been used for the comparison of the two structures. The bridge between the two  $[\text{MoFe}_3\text{S}_4]^{12+}$  species defines a  $\text{Fe}_2\text{S}_2$  rhomb with a short Fe–Fe distance of 2.6692(6) Å only slightly longer than that of clusters **IIb** and **IIc** (at 2.659(15) Å and 2.6512(17) Å, respectively). The M–M distances in cluster **I** are slightly increased compared to those in cluster **II** indicating an expansion of each  $\text{MoFe}_3\text{S}_4$  cubane that is evident by the Mo–Mo distances at 7.931(1) Å compared to those of clusters **IIb** and **IIc** at 7.864(2) and 7.849(2) Å, respectively. The average Mo–Fe distance in **I** is found at 2.719(4) Å (range: 2.703(2)–2.732(2) Å) whereas those in clusters **IIb** and **IIc** are found at 2.677(5) Å (range: 2.658(2)–2.695(2) Å), and 2.665(10) Å (range: 2.6479(11)–2.6815(10) Å), respectively. The average intracubane Fe–Fe distances of **I** are at 2.7355(5) Å (range: Fe–Fe, 2.7040(5)–2.7944(5) Å) compared to those of clusters **IIb** and **IIc** at 2.639(3) Å (range: Fe–Fe, 2.632(2)–2.649(3) Å) and 2.622(5) Å (range: Fe–Fe, 2.6127(13)–2.6302(13) Å), respectively.

The Mo atom has an octahedral geometry with an average Mo–S distance at 2.3652(6) Å (range: Mo–S, 2.3515(6)–2.3923(6) Å) and a Mo–P distance at 2.5967(7) Å. The arrangement of the ligands around the Mo atom is different in cluster **I** compared to clusters **IIb** and **IIc**. In clusters **IIb** and **IIc**, the  $\text{Cl}_4$ -catecholate ligands are parallel to the plane defined by the  $\text{MoFe}_6\text{S}_2$  rhombic unit ( $\text{Fe}_b$  = the iron atom without a terminal ligand) whereas in cluster **I** it is almost perpendicular, Figure 3. This difference indicates that the exchange of the phosphine ligands of the Fe atoms with the borohydride ones is not a simple substitution reaction. It affects the coordination around the Mo atom since bond breaking and formation is required to accommodate the new

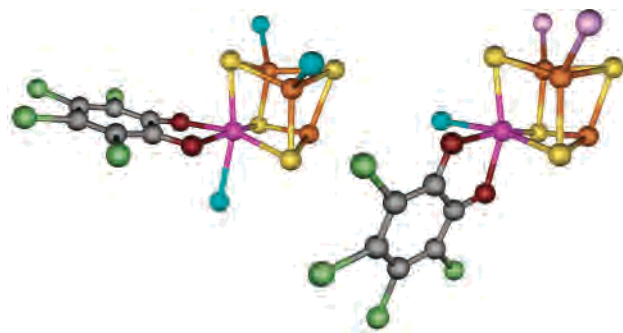


**Figure 3.** Partial view of clusters **IIb** and **I** demonstrating the difference in arrangement around the Mo atom. (Only half of the cluster is depicted in these drawings; the carbon atoms of the phosphines and the  $\text{Bu}_4\text{N}^+$  have been omitted for clarity.)

orientation of the  $\text{Cl}_4$ -catecholate ligands. Each of the Fe atoms (except the two that define the  $\text{Fe}_2\text{S}_2$  rhomb) is also coordinated by an  $\eta^2\text{-BH}_4^-$  bidentate anion as is evident in Figure 2.

The substitution of the phosphine ligands with the borohydrides affects the reduction potential of the final product. The cyclic voltammetry of cluster **I** exhibits a single reduction at  $-743$  mV<sup>10</sup> compared to that of cluster **IIa** at  $-839$  mV. Moreover the reduction of **I** is quasireversible unlike that of **IIa** which is reversible. The electrochemistry hints at the possible formation of a different product after the one-electron reduction. The oxidation states of the metal centers are not affected by the substitution reaction, and that is supported by the EPR spectra (frozen THF) of **I** which are silent like that of **IIa**. Moreover, the magnetic behavior of **I** is comparable to that of **IIa**. Characteristically, the magnetic moments at 2, 5, and 300 K are 5.58, 6.78, and 7.32  $\mu_B$ , respectively.

The IR spectrum at the B–H stretching region<sup>8</sup> is indicative of a bidentate binding mode,<sup>11</sup> but the  $139$   $\text{cm}^{-1}$  separation between the  $\nu_{\text{B-H}}$  (terminal) and  $\nu_{\text{B-H}}$  (bridging) modes is rather small. That is suggestive of a rather weak M– $\text{BH}_4$  interaction. This is confirmed by the X-ray crystal structure where the average Fe– $\text{H}_b$  distances are rather long at 1.903 Å (range: 1.821–1.977 Å). The B–H distances and H–B–H angles reveal an almost ideal tetrahedral arrangement around the boron atom. The  $\text{BH}_4$  unit occupies, through two bridging hydrogens, two coordination sites around irons, but it is thereby forced to an average very small H–Fe–H bite angle of  $51.55^\circ$ . The Fe–B distances are at 2.289(3) Å and at 2.319(3) Å. The  $\text{BH}_4^-$  does not act either as a reducing agent or a source of hydride but rather as a ligand that replaces the terminal phosphines of the four Fe atoms in a ligand substitution reaction. Compound **I** might provide an excellent starting material for biologically relevant metallo–sulfur–hydrido clusters. Preliminary reactivity studies have shown that the  $\text{BH}_4^-$  ligands can be removed in

(9) Crystals suitable for X-ray diffraction were grown for compound **I** (crystal dimensions (mm): 0.40, 0.36, 0.34). Data were collected on a Bruker SMART CCD-based X-ray diffractometer operated at 150 K ( $2\theta_{\text{max}} = 57.99^\circ$ ). The space group ( $P2_1/c$ , monoclinic) was determined on the basis of systematic absences and intensity statistics. Cell dimensions (Å, deg) are  $a = 17.1420(19)$  Å,  $b = 22.604(3)$  Å,  $c = 17.2955(18)$  Å with  $\beta = 110.387(2)^\circ$ , and the volume is  $V = 6282.0(12)$  Å<sup>3</sup>. All hydrogen atoms of the borohydride ligands were located and refined with isotropic thermal parameters. Full-matrix least-squares refinement based on  $F^2$  converged to an R1 [ $I > 2\sigma$ ] value of 0.0330 and a wR2 value of 0.0820, GOF 1.026.

(10) All the cyclic voltammetry experiments were carried out with Pt working and Ag/AgCl reference electrode with 0.1 M of  $^n\text{Bu}_4\text{NPF}_6$  electrolyte in 1,2-dichloroethane. The redox potentials are reported vs SCE.

(11) (a) Marks, T. J.; Kennelly, W. J.; Kolb, J. R.; Shimp, L. A. *Inorg. Chem.* **1972**, *11*, 2540. (b) Marks, T. J.; Kolb, J. R. *Chem. Rev.* **1977**, *77*, 263.

## COMMUNICATION

the presence of an acid (even a weak one such as MeOH) with the simultaneous evolution of H<sub>2</sub> gas, or a base. The compound remains stable in a THF solution for a prolonged period of time in ambient temperatures but loses BH<sub>4</sub><sup>-</sup> or BH<sub>3</sub> upon heating (the B–H stretching vibrations were absent in the IR spectra). Moreover, reaction of **I** with Lewis bases such as diglyme results in the removal of BH<sub>3</sub> by the possible formation of a diglyme: BH<sub>3</sub> adduct. It is not clear if a metal hydride species is formed since this could not be identified by spectroscopic means. NMR studies for example have not been conclusive so far, most likely due to the presence of multiple paramagnetic centers. The isolation and identifica-

tion of these species could be of extreme importance and are the focus of ongoing synthetic attempts in our lab.

**Acknowledgment.** We thank Jeff Campf for X-ray data collection. The authors acknowledge the support of this work by a grant from the National Institutes of Health (GM 33080).

**Supporting Information Available:** X-ray crystallographic file in CIF format for [(Cl<sub>4</sub>-cat)(PPr<sub>3</sub>)MoFe<sub>3</sub>S<sub>4</sub>(BH<sub>4</sub>)<sub>2</sub>](Bu<sub>4</sub>N)<sub>4</sub>. This material is available free of charge via the Internet at <http://pubs.acs.org>.

IC049275W